

Supplementary Material Table of Contents

Supplementary Figure 1. Effects of DRA_{inh}-A270 on oxalate and fluorescein sulfonic acid (FSA) transport, and electrical resistance.

Supplementary Figure 2. Loop fluid volume in the intestinal oxalate absorption study, effects of DRA_{inh}-A270 on mannitol transport, and urine oxalate and creatinine concentrations in the acute oxalate loading study.

Supplementary Figure 3. Urine oxalate and creatinine concentrations in the high-oxalate diet study.

Supplementary Figure 4. DRA_{inh}-A270 selectivity against slc26a1 and slc26a2.

Supplementary Figure 5. DRA_{inh}-A270 inhibition of human SLC26A3.

Supplementary Figure 6. Toxicity and off-target studies in mice.

Supplementary Figure 7. Oxalate standard curve in aqueous solution.

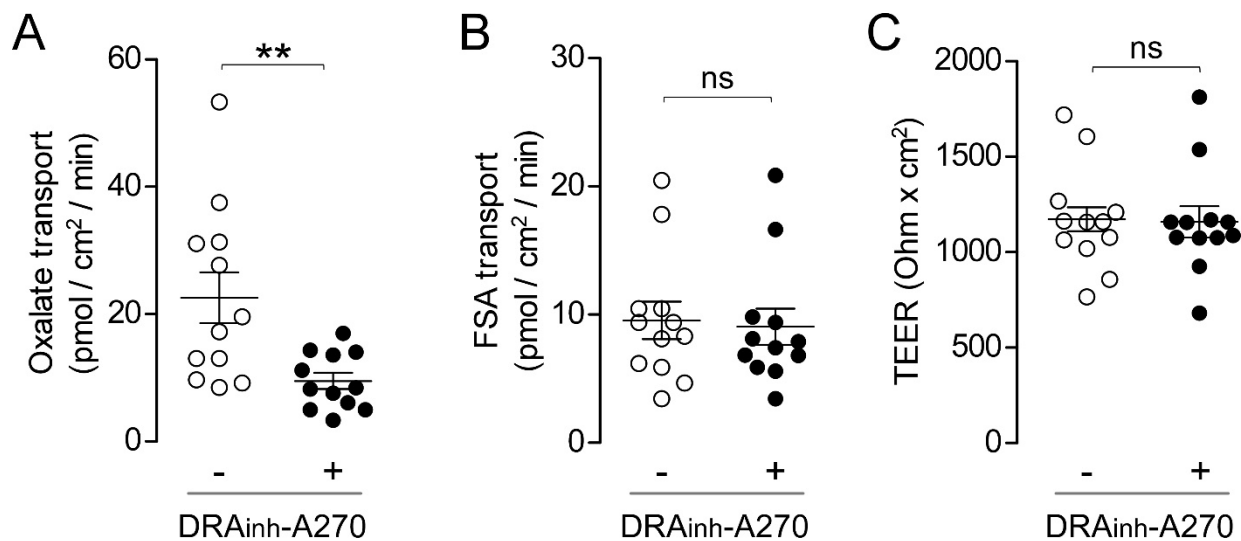
Supplementary Table 1. Eurofins SafetyScreen44 panel results for DRA_{inh}-A270

Supplementary Table 2. CYP450 inhibition of DRA_{inh}-A270 showing mean inhibition for each isoform.

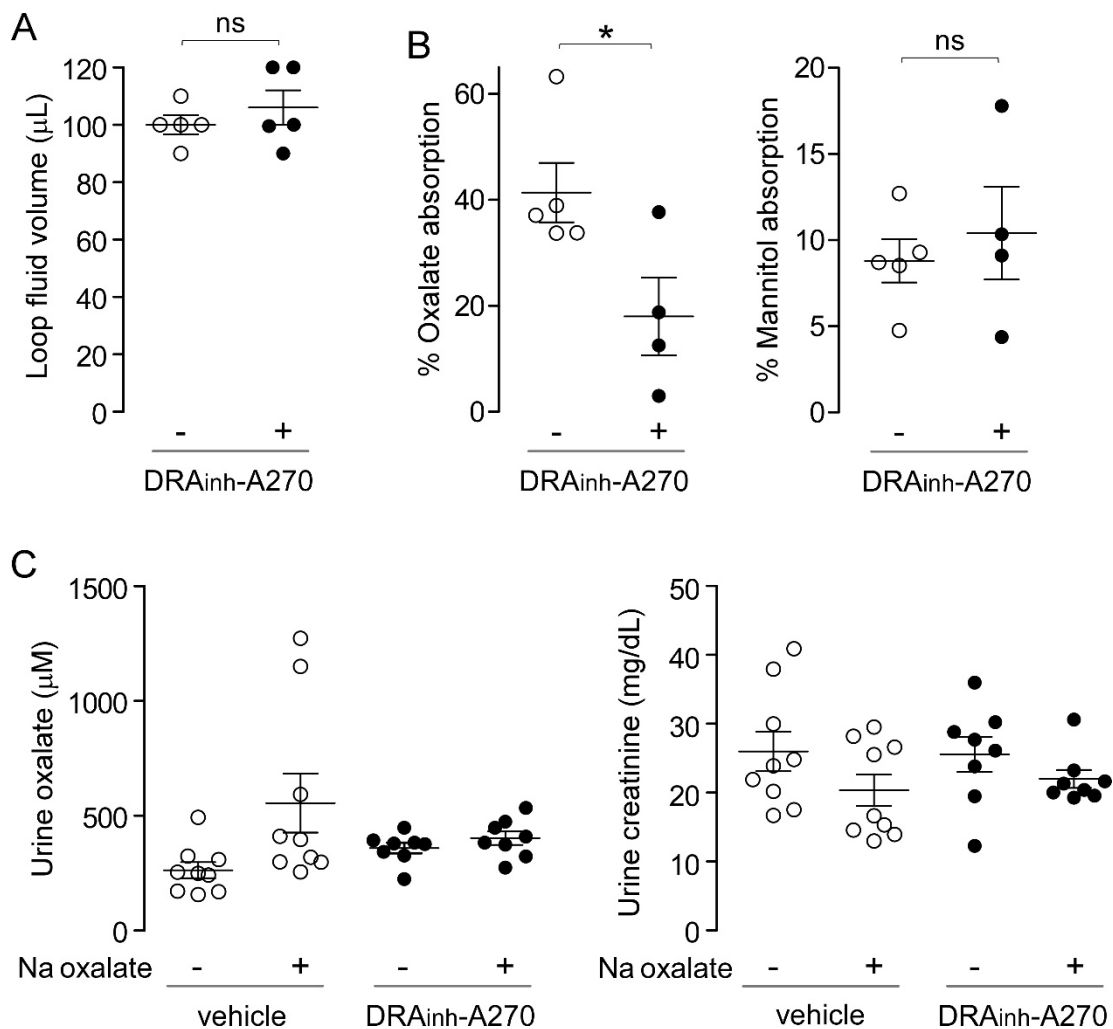
Supplementary Table 3. hERG activity.

Supplementary Table 4. Microsomal stability of DRA_{inh}-A270 in mouse, rat and human liver microsomes.

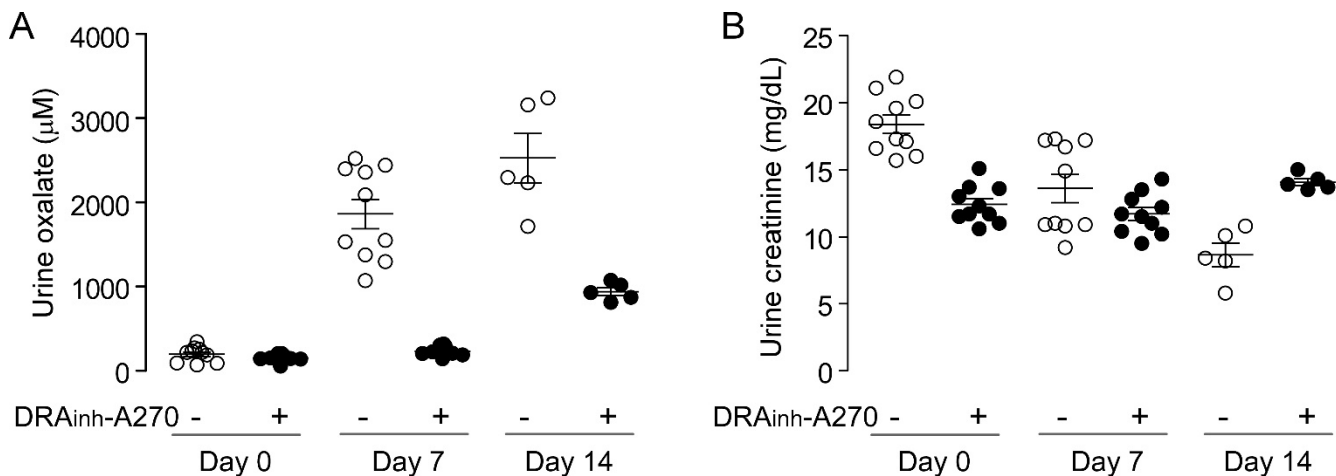
Supplementary Table 5. CBC, serum electrolytes, anion gap and chemistries in mice (on regular diet) treated with DRA_{inh}-A270 (10 mg/kg) or vehicle twice daily for 7 days.



Supplementary Figure 1. Effects of DRA_{inh}-A270 on oxalate and fluorescein sulfonic acid (FSA) transport, and electrical resistance. Oxalate (A) and FSA (B) transport rates in FRT cells expressing SLC26A3 (FRT-A3) pretreated with 10 μ M DRA_{inh}-A270 (or DMSO control) for 15 min prior to application of a 500 μ M oxalate and 200 μ g/mL (\sim 420 μ M) FSA gradient (basolateral-to-apical), as shown in Fig. 1D. C. Transepithelial electrical resistance (TEER) in cells treated with 10 μ M DRA_{inh}-A270 or DMSO control. Mean \pm S.E.M., n=12 wells per group. Student's t-test, **p<0.01, ns: not significant.

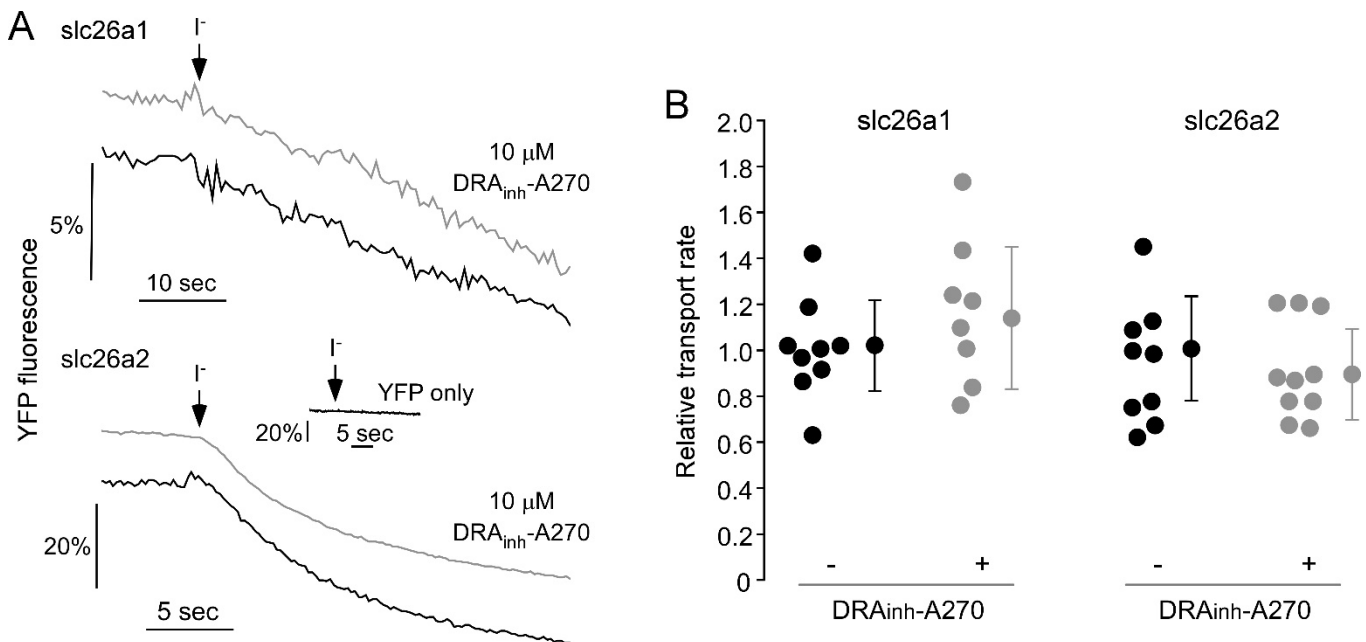


Supplementary Figure 2. Loop fluid volume in the intestinal oxalate absorption study, effects of DRA_{inh}-A270 on mannitol transport, and urine oxalate and creatinine concentrations in the acute oxalate loading study. **A.** Loop fluid volume at 60 min in mouse distal colonic loops injected at 0 min with 100 μ L of Cl⁻-free HEPES-buffered saline containing 500 μ M sodium oxalate (+20 μ M amiloride) with and without 10 μ M DRA_{inh}-A270. N=5 loops per group. **B.** Percentage absorption of luminal oxalate and mannitol (500 μ M each, at 0 min) in mouse distal colonic loops at 60 min in the presence and absence of 10 μ M DRA_{inh}-A270. N=4-5 loops per group. **C.** Urine oxalate (left) and creatinine (right) concentration in mice (CD1 strain) before and after oral Na oxalate loading (2.5 μ mol/kg) and treated with DRA_{inh}-A270 (10 mg/kg, ip) or vehicle at the time of oxalate loading. N=8-9 mice per group. Mean \pm S.E.M., Student's t-test, *p<0.05, ns: not significant.

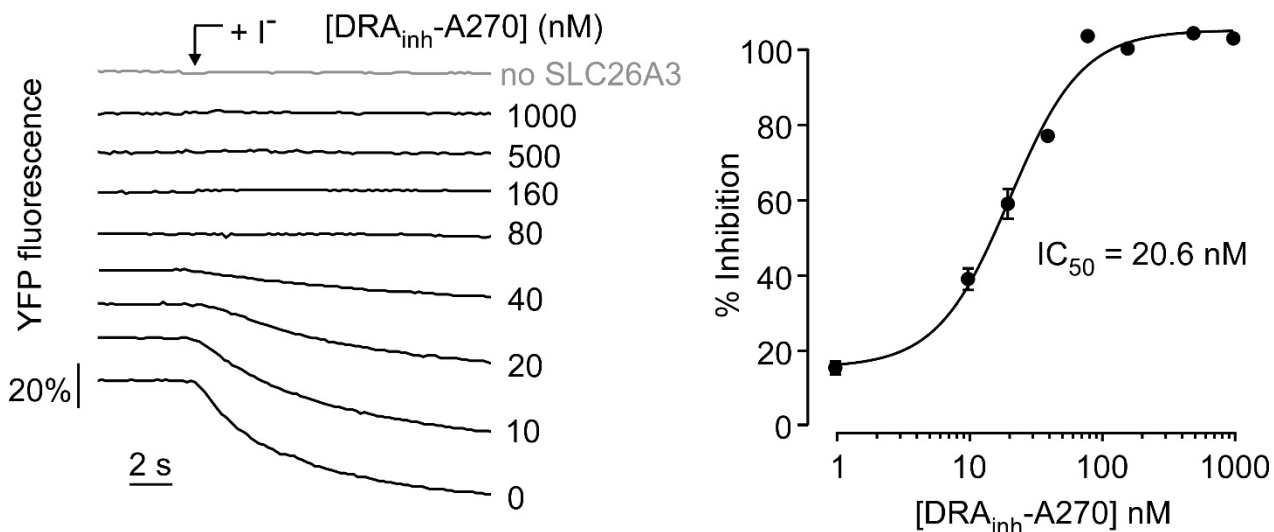


Supplementary Figure 3. Urine oxalate and creatinine concentrations in the high-oxalate diet

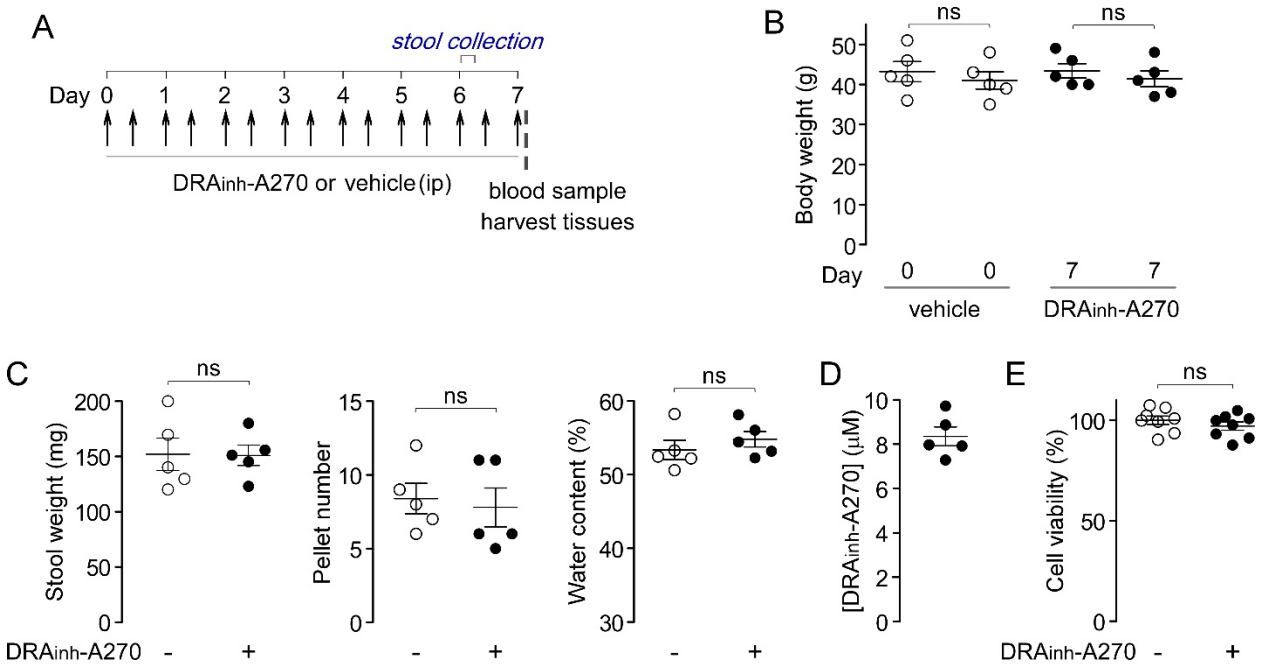
study. A. Urine oxalate concentration in mice (C57BL/6 strain) on Days 0, 7 and 14 of the high-oxalate, low-calcium diet and treated with DRA_{inh}-A270 (10 mg/kg, ip, BID) or vehicle. **B.** Urine creatinine concentration in mice on Days 0, 7 and 14 of the high-oxalate, low-calcium diet and treated with DRA_{inh}-A270 (10 mg/kg, ip, BID) or vehicle. Mean \pm S.E.M., N=5-10 mice per group per time point.



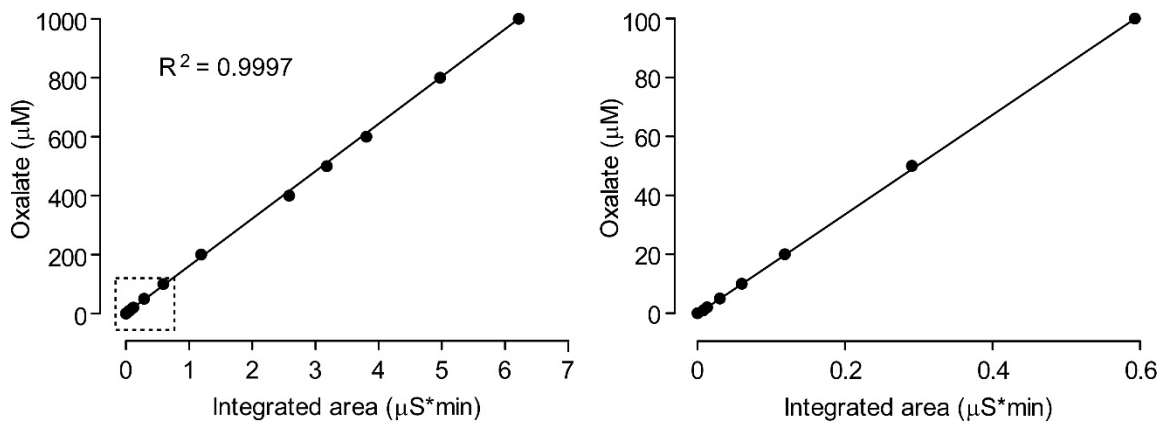
Supplementary Figure 4. DRA_{inh}-A270 selectivity against slc26a1 and slc26a2. A. 293 T/17 cells were transiently transfected with a plasmid to co-express slc26a1 or slc26a2 and a halide-sensitive YFP. Cl⁻/I⁻ exchange activity shown without and with 10 μ M DRA_{inh}-A270. **B.** Summary of relative transport activity for slc26a1 and slc26a2 without and with DRA_{inh}-A270. N=8-10 experiments per condition, mean \pm S.E.M, differences not significant.



Supplementary Figure 5. DRA_{inh}-A270 inhibition of human SLC26A3. (left) 93 T/17 cells were transiently transfected to co-express human SLC26A3 and a halide-sensitive YFP. YFP fluorescence shown as a measure of Cl⁻/I⁻ exchange in the presence of indicated concentrations of DRA_{inh}-A270. The top curve shows FRT-null cells as negative control. (right) Summary data for DRA_{inh}-A270 inhibition of human SLC26A3. Mean \pm S.E.M., n=10-32 cells per data point.



Supplementary Figure 6. Toxicity and off-target studies in mice. **A.** Experimental protocol. **B.** Effect of 7-day DRA_{inh}-A270 (10 mg/kg, ip, twice daily) or vehicle treatment on body weight, n=5 mice per group. **C.** 3-hour stool weight, pellet number and water content at Day 6 in mice treated with DRA_{inh}-A270 or vehicle per panel A, n=5 mice per group. **D.** DRA_{inh}-A270 concentration in plasma at 3 h after the final DRA_{inh}-A270 dose in mice treated for 1 week as in A, n=5 mice. **E.** In vitro cytotoxicity of DRA_{inh}-A270 (10 μM with 24 h incubation) measured by Alamar Blue assay in FRT cells, 0.1% DMSO was used as vehicle (negative) control. N=8 wells per group. As a positive control 20% DMSO reduced cell viability to 16±0.6 % (not shown). Mean ± S.E.M., unpaired t-test, ns: not significant.



Supplementary Figure 7. Oxalate standard curve in aqueous solution. Integrated area of oxalate peak ($\mu\text{S}^*\text{min}$) for aqueous solutions (phosphate-buffered saline) containing specified concentrations of sodium oxalate. The graph on the right is an expansion of the dashed rectangular area on the left.

Supplementary Table 1. Eurofins SafetyScreen44 panel results for DRA_{inh}-A270. Assays were done in duplicate with 10 μ M DRA_{inh}-A270, mean % inhibition is shown.

Assay name	Inhibition (%)
5-HT1A Human Serotonin GPCR Binding (Agonist Radioligand) Assay	0
5-HT1B Human Serotonin GPCR Binding (Antagonist Radioligand) Assay	-1
5-HT2A Human Serotonin GPCR Binding (Antagonist Radioligand) Assay	17
5-HT2B Human Serotonin GPCR [³ H]LSD Binding (Agonist Radioligand) Assay	64
5-HT3 Human Serotonin Ion Channel Binding (Antagonist Radioligand) Assay	-6
A2A Human Adenosine GPCR Binding (Agonist Radioligand) Assay	46
Acetylcholinesterase Human Enzymatic Assay	10
alpha1A Human Adrenoceptor GPCR Binding (Antagonist Radioligand) Assay	5
alpha2A Human Adrenoceptor GPCR Binding (Antagonist Radioligand) Assay	47
AR Human Androgen NHR Binding (Agonist Radioligand) Assay	13
beta1 Human Adrenoceptor GPCR Binding (Antagonist Radioligand) Assay	14
beta2 Human Adrenoceptor GPCR Binding (Antagonist Radioligand) Assay	3
Cav1.2 (L-type) Rat Calcium Ion Channel Binding (Dihydropyridine Site) Assay	-6
CB1 Human Cannabinoid GPCR Binding (Antagonist Radioligand) Assay	-3
CB2 Human Cannabinoid GPCR Binding (Agonist Radioligand) Assay	-1
CCK1 (CCKA) Human Cholecystokinin GPCR Binding (Agonist Radioligand) Assay	-5
COX1 Human Cyclooxygenase Enzymatic Assay	-1
COX2 Human Cyclooxygenase Enzymatic Assay	15
D1 Human Dopamine GPCR Binding (Antagonist Radioligand) Assay	13
D2S Human Dopamine GPCR Binding (Antagonist Radioligand) Assay	2
DAT Human Dopamine Transporter Binding (Antagonist Radioligand) Assay	-2
delta (DOP) Human Opioid GPCR Binding (Antagonist Radioligand) Assay	-3
ETA Human Endothelin GPCR Binding (Agonist Radioligand) Assay	13
Glutamate (NMDA, Non-Selective) Rat Ion Channel [³ H] CGP-39653 Binding Assay	16
GR Human Glucocorticoid NHR Binding (Agonist Radioligand) Assay	-7
H1 Human Histamine GPCR Binding (Antagonist Radioligand) Assay	27
H2 Human Histamine GPCR Binding (Antagonist Radioligand) Assay	-2
hERG Human Potassium Ion Channel [³ H] Dofetilide Binding (Antagonist Radioligand) Assay	19
kappa (KOP) Human Opioid GPCR Binding (Antagonist Radioligand) Assay	7
KV (Non-Selective) Rat Potassium Ion Channel [¹²⁵ I] alpha-Dendrotoxin Binding Assay	-1
M1 Human Acetylcholine (Muscarinic) GPCR Binding (Antagonist Radioligand) Assay	9
M2 Human Acetylcholine (Muscarinic) GPCR Binding (Antagonist Radioligand) Assay	-3
M3 Human Acetylcholine (Muscarinic) GPCR Binding (Antagonist Radioligand) Assay	8
Monoamine Oxidase A (MAO-A) Human Enzymatic Assay	73
mu (MOP) Human Opioid GPCR Binding (Antagonist Radioligand) Assay	-5
nAChR (alpha4/beta2) Human Ion Channel Binding (Agonist Radioligand) Assay	-3
NET Human Norepinephrine Transporter Binding (Antagonist Radioligand) Assay	29
Non-Selective Rat GABAA Ion Channel [³ H] Flunitrazepam Binding (Agonist Radioligand) Assay	-8
Non-Selective Rat Sodium Ion Channel [³ H] Batrachotoxinin Binding (Site 2) Assay	22
PDE3A Human Phosphodiesterase Enzymatic Assay	4
PDE4D2 Human Phosphodiesterase Enzymatic Assay	-2
SET Human Serotonin Transporter Binding (Antagonist Radioligand) Assay	-7
V1A Human Vasopressin / Oxytocin GPCR Binding (Antagonist Radioligand) Assay	-1

Supplementary Table 2. CYP450 inhibition by DRA_{inh}-A270 showing mean inhibition for each isoform. CYP450 activity was measured in human liver microsomes in the presence and absence of 10 μ M DRA_{inh}-A270 (n=2 per condition). Substrates for each isoform: CYP1A2: phenacetin (30 μ M); CYP2C9: diclofenac (10 μ M); CYP2C19: S-mephénytoïn (35 μ M); CYP3A4: midazolam (5 μ M) and testosterone (80 μ M); CYP2D6: bufuralol (10 μ M); CYP2C8: paclitaxel (10 μ M); CYP2B6: bupropion (70 μ M). Positive controls (reference) were: CYP1A2: α -maphthoflavone; CYP2C9: sulfaphenazole; CYP2C19: omeprazole; CYP3A4: ketoconazole; CYP2D6: quinidine; CYP2C8: nicardipine; CYP2B6: clopidogrel.

Compound	% of CYP inhibition (mean)							
	1A2	2B6	2C8	2C9	2C19	2D6	3A4 (midazolam)	3A4 (testosterone)
Reference	100	95.6	97.1	92.8	96	83.5	98.4	95.5
DRA _{inh} -A270	11.4	55.6	49.9	18.2	5.3	24.3	-20.5	-11.9

Supplementary Table 3. hERG activity. hERG activity ($n \geq 2$ per condition) was measured by manual patch-clamp in Chinese Hamster Ovary cells stably transfected with hERG. Cisapride (0.1 μ M) was used as positive control Mean \pm S.D., $n=2-4$ experiments per group.

Compound	% hERG inhibition
DRA _{inh} -A270	1.9 \pm 4.6
cisapride	93.9 \pm 0.4

Supplementary Table 4. Microsomal stability of DRA_{inh}-A270 in mouse, rat and human liver microsomes. DRA_{inh}-A270 was incubated in the reaction mixture with NADPH for 0, 5, 15, 30 and 45 min at 37°C in duplicate with final liver microsomal protein concentration of 0.5 mg/mL. DRA_{inh}-A270 concentration was measured at each time point by LC-MS/MS and in vitro elimination half-life was calculated. Ketanserin was used as the reference compound with rapid metabolism.

Test compound	Species	Percent remaining (%)					T _{1/2} (minutes)
		0 min	5 min	15 min	30 min	45 min	
ketanserin	human	100	88.4	69.1	49.4	39.9	33.40
	rat	100	68.9	36.5	16.1	6.9	11.86
	mouse	100	82.1	54.4	30.8	19.5	18.94
DRA _{inh} -A270	human	100	94.9	102.5	95.7	102.5	∞
	rat	100	97.9	91.8	96.3	95.1	876.17
	mouse	100	99.1	96.5	84.1	88.8	201.23

Supplementary Table 5. CBC, serum electrolytes, anion gap and chemistries in mice (on regular diet) treated with DRA_{inh}-A270 (10 mg/kg) or vehicle twice daily for 7 days. Mean ± S.E.M., unpaired t-test, n=5 mice per group.

	vehicle	DRA_{inh}-A270	P value
Hemoglobin (g/dL)	14.6±0.1	14.8±0.2	>0.05
Hematocrit (%)	55.7±0.4	56.8±0.8	>0.05
WBC (10 ³ /µL)	7.4±1.2	6.6±1.7	>0.05
Platelets (10 ³ /µL)	739±21	812±36	>0.05
Sodium (mmol/L)	156.0±0.5	154.6±0.6	>0.05
Potassium (mmol/L)	5.1±0.4	4.8±0.1	>0.05
Chloride (mmol/L)	118±0.3	116±0.7	>0.05
Bicarbonate TCO ₂ (mmol/L)	15±1.1	16±1.0	>0.05
Anion gap (mmol/L)	22±1.9	23±1.6	>0.05
Calcium (mg/dL)	8.3±0.1	8.4±0.1	>0.05
Phosphorus (mg/dL)	7.2±0.4	6.9±0.4	>0.05
Creatinine (mg/dL)	0.04±0.02	0.06±0.02	>0.05
BUN (mg/dL)	15±0.9	13±1.3	>0.05
Total protein (g/dL)	4.5±0.02	4.4±0.1	>0.05
Albumin (g/dL)	2.5±0.04	2.4±0.05	>0.05
Globulin (g/dL)	2.0±0.02	2.0±0.04	>0.05
Total bilirubin (mg/dL)	0.3±0.03	0.3±0.03	>0.05
Bilirubin - unconjugated (mg/dL)	0.1±0	0.08±0.2	>0.05
Bilirubin - conjugated (mg/dL)	0.20±0.03	0.22±0.02	>0.05
Glucose (mg/dL)	175±7.8	156±9.7	>0.05
ALT (U/L)	56±14	40±7	>0.05
AST (U/L)	83±4	76±11	>0.05
ALP (U/L)	65±5	70±4	>0.05
Creatine kinase (U/L)	603±72	431±96	>0.05
Cholesterol (mg/dL)	112±5	98±10	>0.05